



Preparation of cellulose fiber derived from sugarcane bagasse and polyvinyl alcohol (PVA)-based hydrogel composite by gamma irradiation as a platform for colorimetric sensor

Nattawan Khiewswai¹ · Thitirat Rattanawongwiboon² · Chonnipha Tangwongputti² · Sarute Ummartyotin^{1,3}

Received: 29 August 2023 / Accepted: 20 October 2023 / Published online: 11 November 2023
© Qatar University and Springer Nature Switzerland AG 2023

Abstract

Cellulose fiber was successfully extracted and purified from sugarcane bagasse by using an alkali treatment process and bleaching. It was employed to use as a reinforcement part in polyvinyl alcohol (PVA) and polyethylene glycol diacrylate composite (PEGDA). The weight ratio of cellulose and PVA was set to 1:1. Gamma irradiation technique with various doses ranging from 10 to 50 kGy was employed. The presence of C-H stretching, O-H stretching, and C=O stretching was observed. Less intensity of X-ray diffraction was observed, suggesting that cellulose was embedded into the polymer blend matrix. It was thermally stable at 200 °C. The compressive strength was in the range of 10–20 MPa. By using a low irradiation dose, gel fraction was less, while swelling behavior and porosity were relatively high. A total of 85–90% of gel fraction, 100–300% of swelling behavior, and 95–97% of porosity were observed. The morphological properties exhibited as a porous network. The role of methyl red was employed as a color agent to react with volatile gas. The color was changed from red to yellow with respect to the increment of time. The characteristic peaks of 425 nm and 525 nm were observed due to yellow and red color, respectively. Preliminary test of hydrogel composite as a platform for colorimetric sensor was tested for durian ripeness. It was remarkably noted that hydrogel composite prepared by gamma irradiation technique was considered as an excellent candidate material for food sensory prediction.

Keywords Cellulose · Hydrogel · Sugarcane bagasse · Colorimetric sensor · Ripeness indicator · PVA

Highlight

- (1) Cellulose was successfully extracted and purified from sugarcane bagasse.
- (2) Cellulose and PVA-based hydrogel were formed by PEGDA as a cross-linking agent.
- (3) It was operated under 10, 20, 30, 40, and 50 kGy of gamma ray irradiation's doses.
- (4) It was employed as a colorimetric sensor for food spoilage indicator.

✉ Thitirat Rattanawongwiboon
thitirat@tint.or.th

✉ Sarute Ummartyotin
sarute@tu.ac.th

¹ Department of Materials and Textile Technology, Faculty of Science and Technology, Thammasat University, Pathum Thani 12120, Thailand

² Thailand Institute of Nuclear Technology (Public Organization), Ongkharak, Nakhon Nayok 26120, Thailand

³ Center of Excellence on Petrochemical and Materials Technology, Chulalongkorn University, Bangkok 10330, Thailand

1 Introduction

In recent year, Thailand was considered as one of the largest countries for agricultural production and consumption. The agricultural activities were versatile in various sectors starting from farm to factory. It was typically related to upstream, midstream, and downstream processes. The activities were versatile such as cultivation, postharvest, packaging as well as logistic. The main purpose of activities related to agriculture was to ensure the excellent quality of product from farm to table. In the Thai market, numerous agricultural products were produced from local form such as palm oil, rice, pineapple as well as sugarcane. It can be not only produced for domestic consumption but also be exported to overseas countries. One of the most abundant products was typically related to sugarcane. To the best of the author's knowledge, it was structurally defined as a perennial grass with a size of 2–4 m [1]. It was commonly considered as a raw material for sugarcane production. It was commonly employed as a food and dessert ingredient. Although sugar

effectively provided the benefits in terms of the food science, the process of sugar production was still limited in particular cases such as uncontrollable price, lack of product quality, and insufficient product for consumption. By virtue of these reasons, it significantly provided the difficulty for sugar production. Furthermore, with the exponential growth of the worldwide population and economy, the growth of sugar production was therefore presented as a footprint. The bagasse was continuously occurred in order of magnitude. With a high amount of bagasse, it was therefore provided the difficulty to manage. It exhibited as a residual and waste. The existence of bagasse was thus useless. Without technical knowledge, it was undergone by the combustion process. It was consequently occurred as an environmental pollutant to soil, water, and air. With this regard, it was considered as a hazardous process for the environment. In order to overcome this limitation, the use of bagasse with higher efficiency was considered as one of the most strategies for environmental remediation. From the structural point of view, sugarcane bagasse was mainly composed of cellulose fiber [2]. It was presented as a lignocellulosic fiber with randomly distributed as fibrous network, lignin and other impurities [3]. With this regard, cellulose can be chemically extracted and purified from sugarcane bagasse. Without lignin and impurities, purified cellulose illustrated many outstanding properties such as excellent mechanical properties and high thermal and chemical stability. It can be therefore offered the great promise for various applications including reinforcement part in composite [4], electronic paper/packaging [5], catalyst [6] as well as platform for chemical sensor [7, 8]. Recently, Chopra et al. [9] investigated the extraction process of cellulosic fibers from the natural resources such as rice husks, wood pulp, banana peels, coffee husks, wheat straw, sisal fibers, and bagasse. It was remarkable to note that cellulose fiber exhibited the excellence of biodegradability and non-toxicity. To use cellulose from naturally occurring resource was therefore considered as one of the most attractive strategies for environmental remediation. After that, Sriwong et al. [10] evaluated the fabrication of a bio-based composite prepared from cellulose fiber and hydroxyapatite. Cellulose was successfully extracted from sugarcane bagasse with higher purity and homogeneity. The existence of hydroxyapatite powder was to enhance the proliferation, attachment, and differentiation of preosteoblast cells for tissue engineering. It was considered as an excellent candidate for scaffold material. Up to the present time, research of cellulose extraction process from sugarcane bagasse was therefore encouraged.

To the best of the authors' knowledge, cellulose was typically considered as a polysaccharide-based material. It was regarded as an organic compound with an empirical formula of $(C_6H_{10}O_5)_n$. It was structurally defined as a linear chain of β (1 \rightarrow 4) linked D-glucose units [11] with a high level of molecular weight. It was a randomly oriented

network. The porosity was therefore created by the repulsive force of hydroxyl groups alongside of its fiber. Moreover, the utilization of cellulose was strongly encouraged due to its eco-friendly purpose. It was typically related to "green policy". The use of product and process with eco-friendly concept should be preferably supported. One effective route for cellulose utilization was focused on composite development. With the excellent properties of cellulose, it offered the attractiveness for many applications based on composite design. Although polymer-based materials provided the excellent properties in terms of engineering usage, it was still limited due to inferiority of dimensional stability and thermal resistance. The existence of cellulose in a polymer-based matrix can overcome these technical issues. With the presence of cellulose, it was facile to degrade within the controllable timeframe. It was therefore considered as an eco-friendly and sustainable material.

For the design of a cellulose-based polymeric composite, PVA was commonly employed as a hydrogel-based material. It was regarded as a water-soluble synthetic polymer with the formula of $[CH_2CH(OH)]_n$. Nevertheless, it was eco-friendly to the environment, but it was limited in particular use such as low thermal and dimensional stability. As a consequence, the use of PVA was still in trouble when long term of usage was involved. Pristine PVA was easy to be dissolved in solution. In order to overcome these obstacles, the development of cellulose and PVA-based composite hydrogel was considered as an alternative strategy. Recently, Sun et al. [12] developed cellulose and PVA-based hydrogel composite. The presence of cellulose nanocrystal can enhance the mechanical strength of hydrogel. Furthermore, it can be activated by an external stimuli responsiveness. Then, Wu et al. [13] fabricated the conductive hydrogels for stress sensors by cellulose and PVA-based hydrogel composite. The role of cellulose can improve the resistance of mechanical fatigue and swelling behavior in composite. Interestingly, the role of cellulose can be used to enhance the mechanical properties of PVA. Fang et al. [14] investigated the influence of cellulose in PVA hydrogel composite. Compressive strength, resilience, and biocompatibility of PVA were therefore elevated. Baniasadi et al. [15] developed a cellulose and PVA gel-based composite. It can be easily shaped by 3D printing technique. It therefore offered numerous advantages for scaffold material. This is in agreement with Lu et al. [16] work. With the existence of cellulose in PVA composite, it can create the three-dimensional network and offer the superiority in mechanical properties.

Up to the present time, although cellulose-based composite significantly offered many engineering benefits, the processing was typically related to chemical reagents. It was therefore provided the difficulty to control the percent yield of the product. Furthermore, the process related to chemical reagents may involve the volatile solvent and by-product. It was subsequently limited due to ease of corrosion, toxicity to air, and difficulty

to maintain the purity. It was consequently resulted in the difficulty for large-scale mass production. To overcome this technique issue, the utilization of gamma irradiation technique for cellulose-based composite development was encouraged. This strategy offered the great promise for composite fabrication by creating the free radical throughout the polymeric network. To the best of the authors' knowledge, the gamma irradiation process used cobalt 60 radiation for a variety of applications, including sterilization, decontamination, and materials modification [17]. With high energy, it can be activated the polymer chain. It can be initiated the crosslinking reaction between the polymer chain and cellulose to form the composite without any chemical reagents. Kaouach et al. [18] studied the role of gamma irradiation for PEO and PVA based binary blend composite. The compound was prepared with well-ordered spherulites and high pore density. It was therefore obtained high percent yield of product. In Thailand, one of the most important industries was referred to "food industry." The food product, packaging, and sensor were considered as important keys to predict the quality and shelf life. It can create the value to product for domestic consumption and international export. In order to predict the quality of food products, colorimetric sensor was remarkably noted as the most important strategies. It was defined as an analytical technique for the determination of concentration of a chemical compound with the aid of a color reagent. Up to the present time, cellulose derived from sugarcane bagasse-based hydrogel for colorimetric platform has extensively developed.

The objective of this work was to develop cellulose and PVA-based hydrogel composite by gamma irradiation technique. The novelty of this work is to prepare a cellulose-based PVA/PEGDA blend composite by gamma irradiation technique. Cellulose was extracted and purified from sugarcane bagasse by alkali treatment. PEGDA was also integrated for dimensional stability. Various gamma irradiation doses ranging from 10 to 50 kGy were studied. Physico-chemical properties of cellulose-based hydrogel composite were therefore evaluated. After that, the preliminary test as a colorimetric sensor was therefore evaluated.

2 Materials and methods

2.1 Materials and Chemical reagents

Sugarcane bagasse was supplied from a local sugar factory (Thailand). Sodium hydroxide (NaOH; molar mass = 40 g/mol) and acetic acid (CH₃COOH; molar mass = 60.05 g/mol) were purchased from Merck Chemical, Co., Ltd. (Germany). Sodium chlorite (NaClO₂) was purchased from DC Fine Chemicals, Co., Ltd. (Spain). PVA (Mw = 145,000 Da) was purchased from Fluka Analytical, Co., Ltd. (USA). PEGDA (Mn = 575) was purchased from Sigma-Aldrich, Co., Ltd. (USA). Methyl

red (MR) was purchased from Daejung Chemicals & Metals, Co., Ltd. (Korea). Ammonia solution (NH₃) was purchased from VWR Chemicals, Co., Ltd. (USA). All of the chemical reagents were used as received without any further purification.

2.2 Methodology

2.2.1 Cellulose extraction and purification from sugarcane bagasse

Cellulose powder was successfully extracted and purified by sugarcane bagasse. It was treated with 0.5 M of NaOH at 80 °C for 4 h in order to remove lignin and hemicellulose. After that, it was washed several times until neutral pH. The solvent was removed by filtration technique. It was operated by a suction flask which is connected to a vacuum pump. Then, it was bleached with 1.3% w/v of NaClO₂ and 10% v/v of CH₃COOH. The mixture was continuously stirred with DI water and subsequently freeze-dried. It was stored in a desiccator in order to avoid the moisture absorption. Additional information can be found in our previous article [19].

2.2.2 Preparation of cellulose and PVA-based hydrogel composite

To prepare a hydrogel-based composite, the PVA solution and cellulose suspension were mixed. Briefly, 4% w/v of PVA was dissolved into DI water. A total of 4.0% w/v of cellulose suspension was prepared. It was mixed in the weight ratio of 1:1. It was continuously stirred in order to ensure the homogeneity. After that, 0.5% v/v of PEGDA was added in order to form a gel (PVA-cellulose-PEGDA). The sample without PEGDA was also prepared for comparability (PVA-cellulose). Then, it was undergone gamma irradiation technique by using various doses ranging from 10 to 50 kGy.

2.3 Characterization techniques

2.3.1 Fourier transform infrared (FTIR)

FTIR was used to characterize the functional group of samples. The measurement was conducted by using Transmittance Mode. FTIR spectra were obtained in the range of wavenumber from 4000 to 500 cm⁻¹ with a resolution of 2 cm⁻¹ (Invenio ® FTIR spectrometer, Bruker).

2.3.2 X-ray diffraction analysis (XRD)

X-ray diffraction (XRD) was employed to evaluate the crystallinity of the sample. The instrument was conducted under

the guidance of Bruker AXS Model D8 Advance, Germany. X-ray diffractometer was set up by using Cu K α radiations at wavelength 1.54060 Å. The diffraction angle (2 θ) was 5–60°.

2.3.3 Thermogravimetric analysis (TGA)

The thermal decomposition behavior was determined by using a thermogravimetric analyzer (TGA55) from TA Instruments (USA). TGA studies were carried out in a nitrogen atmosphere at a flow rate of 60 mL/min. The temperature was set up from 30 to 600 °C with a heating rate of 10 °C/min.

2.3.4 Scanning electron microscope (SEM)

Morphological properties were investigated by scanning electron microscope (JEOL JSM7800F). Before analysis, the sample was sputter-coated with gold in order to enhance the electrical conductivity. The experiment was set up with the accelerating voltage of 2 kV and magnification of 100 \times .

2.4 Determination of physico-chemical properties of cellulose and PVA-based hydrogel composite

2.4.1 Gel fraction

After irradiation, the samples were cut into four small pieces and air-dried in an oven at 60 °C for 48 h. The dried samples were weighed (W_i), and subsequently, each gel sample was immersed in DI water for 30 min to remove the non-crosslinked PEGDA, followed by lyophilization until a constant weight (W_d). The gel fraction was calculated from Eq. (1):

$$\text{Gel fraction (\%)} = (W_d/W_i) \times 100\% \quad (1)$$

2.4.2 Swelling behavior

To estimate the swelling ratio, a 45 mg dried sample of PVA gels, PVA-PEGDA gels, PVA-cellulose gels, and PVA-cellulose-PEGDA gels was immersed in DI water (20 ml) for 24 h. At different time intervals, the swollen samples were withdrawn and weighed after removing the superficial water using a filter paper. The swelling ratio (SR) was calculated from Eq. (2):

$$\text{Swelling ratio (\%)} = (W_t - W_1)/W_1 \times 100\% \quad (2)$$

where W_1 and W_t represented the weight of the dried sample and the weight of the swollen sample at different time intervals, respectively [20].

2.4.3 Porosity

The porosity of the sample was calculated from Eq. (3):

$$P = [((W_1 - W_2)/\rho_w) \times 100] / [(W_2/\rho_{PVA}) + ((W_1 - W_2)/\rho_w)] \quad (3)$$

where W_1 and W_2 were the weights of the sample before and after drying, respectively. ρ_w was the density of water (1.0 g/cm³), and ρ_{PVA} was the density of PVA (1.19 g/cm³). Additional information of porosity determination equation can be found in the literature of Mahaninia et al. [21].

2.4.4 Mechanical properties

The samples were cylinder-shaped, with a 28 mm diameter and a 10 mm thickness. Compressive strength was done on a universal testing machine (LLOYD) at a crosshead speed of 1 mm/min up and a 50 N load cell equipped with a 50 mm probe. The sulfur compound sensing study used samples with high compressive strength.

2.5 Determination as a colorimetric sensor

2.5.1 Preliminary test as a colorimetric sensor

PVA-cellulose-PEGDA with high-compressive strength hydrogels and suitable gel fractions was prepared as colorimetric sensors. It can be synthesized by adding 1.0 mg of methyl red into PVA-cellulose-PEGDA and irradiation at 40 kGy. The morphological properties of PVA-cellulose-PEGDA-methyl red gels were examined by scanning electron microscopy.

Meanwhile, the UV-vis spectrophotometer (SPECORD® 200 PLUS, WinASPECT) was used to measure the wavelengths of the methyl red solutions at pH ranges of 4.0–7.5. In brief, MR was dissolved into the mixture of the solvent of DI water to ethanol (3:1) by a volume ratio of 25 ppm (25 mg/L). Next, the color changes of the MR solutions in response to NH₃ were evaluated. In brief, an unsealed centrifuge tube was placed into a glass vial, then 1 mL of NH₃ solution (0–1000 ppm) and 5 mL of MR solution, respectively. The glass vial was quickly sealed. The color change of the MR solution was photographed after 30 min with the smartphone.

The PVA-cellulose-PEGDA-methyl red gels were cut into round pieces with a punch plier. After that, the stainless-steel wires were used to suspend the hydrogel in glass vials (20 mL). Followed by the addition of NH₃ solution (200 ppm, 3 mL) through a pipette, and then these vials were quickly sealed. Finally, the hydrogel was photographed every minute using a smartphone. Lastly, color picking software (ImageJ) was used to capture the RGB parameters from the central region of the hydrogel, and the response signal versus time was plotted. The formula for calculating the response signal (S)-based RGB parameters is G/R . Here, R_0 , G_0 , and B_0 were the initial values of the hydrogel indicator, while R , G , and B were the real-time values, and $\Delta R = |R - R_0|$, $\Delta G = |G - G_0|$, $\Delta B = |B - B_0|$. The reference information was from previous research [22].

2.5.2 Application of hydrogels as colorimetric sensors for food spoilage indicator

Fresh durian 350 g was packed in clear rigid polypropylene packaging along with the hydrogels in polyethylene (PE) cups and kept at 35 °C for 7 days, respectively, for the designated period. Fresh durian's physical and chemical were evaluated at the initial intervals of 0, 3, 5, and 7 days, respectively. More detail was available in the previous research [23]. Thereafter, FTIR analysis was performed to evaluate the effect of volatile sulfur on the hydrogel as a colorimetric sensor. Finally, the software (ImageJ) was used to capture the RGB parameters of the hydrogels that color change over time.

3 Results and discussion

3.1 Characterization of cellulose derived from sugarcane bagasse and PVA hydrogel composite

Figure 1 shows the FTIR spectra of cellulose-based composite hydrogel. The pristine cellulose, PVA gels, and PEGDA were provided for comparison. The FTIR spectra of PVA-cellulose gels and PVA-cellulose-PEGDA gels were presented. It exhibited the similar pattern of characteristic peaks. At the wavenumber of 1728 cm^{-1} , this peak was presented due to C-O stretching. It was typically related to the carbonyl group of PEGDA. Furthermore, the broad region of peak at the wavenumber of 3552–2975 cm^{-1} was observed. It was corresponded to O-H stretching. It was referred to as the hydroxyl group. It can be assumed that the presence of the hydroxyl group can be induced to hydrogen bonding throughout the hydrogel network. With the presence of hydrogen bonding, it can be activated by irradiation technique. The major portion of the energy was absorbed by water forming free radicals and molecular products [24], which are shown: $\text{H}_2\text{O} \rightarrow \bullet\text{H}$, $\bullet\text{OH}$, e^- (aq.), H_2O_2 , H_2 , H^+ . A radical with a carbon-centered was created in polymer chains as a result of the radicals OH abstracting hydrogen from the polymer chain. This was typically related to PVA and PEGDA. These carbon-centered radicals on the polymer chain further decay by forming intermolecular crosslinking. It resulted in an increment of molecular weight and forms a three-dimensional network structure [25]. Moreover, it was observed from the intensity range between 3552 and 2975 cm^{-1} of PVA. The intensity of the peak decreased after the addition of cellulose. It can be suggested that hydrogel containing this functional group was very facile to absorb the molecule of water onto its surface. In the case of pristine cellulose, various characteristic peaks were observed at the wavenumber of 3492–3185 cm^{-1} , 2915 cm^{-1} , 1643 cm^{-1} , 1030 cm^{-1} , and 896 cm^{-1} , and these peaks were corresponded to O-H stretching, C-H stretching, O-H

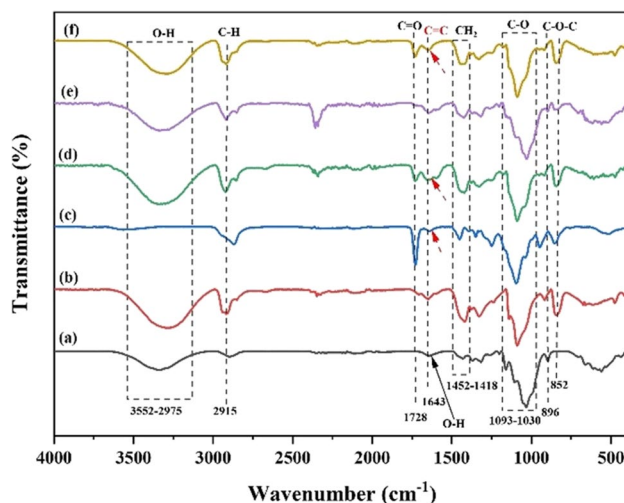


Fig. 1 FTIR spectra of cellulose-based composite hydrogel (a) cellulose, (b) PVA gels, (c) PEGDA, (d) PVA-PEGDA gels, (e) PVA-cellulose gels, and (f) PVA-cellulose-PEGDA gels

bending, C-O bending, and C-C stretching, respectively. These peaks were belonged to the stretching of β -(1–4)-glycosidic linkages. This was considered as monomer unit of cellulose. This was consistent with previous literatures [26, 27]. In the case of PVA gels, the peaks of 3422–3095 cm^{-1} , 1070 cm^{-1} , and 2919 cm^{-1} were observed due to the existence of O-H stretching and symmetric and asymmetric stretching of C-H, respectively. The peak at 1628 cm^{-1} was related to an acetyl group (C=O). A bending vibration related to CH_2 groups was observed in the region of 1454–1425 cm^{-1} [28, 29]. In the case of PEGDA, the characteristic peaks at 2875 cm^{-1} , 1728 cm^{-1} , 1639 cm^{-1} , and 1091 cm^{-1} were observed. These peaks were assigned to C-H stretching, C=O stretching, C=C stretching,

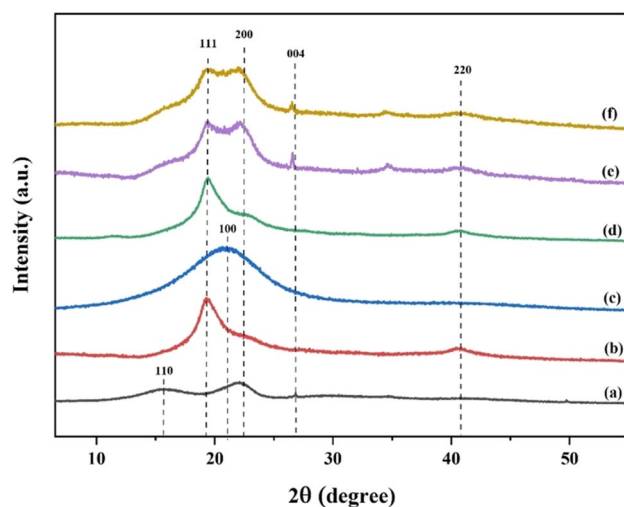


Fig. 2 XRD of cellulose-based composite hydrogel (a) cellulose, (b) PVA gels, (c) PEGDA, (d) PVA-PEGDA gels, (e) PVA-cellulose gels, and (f) PVA-cellulose-PEGDA gels

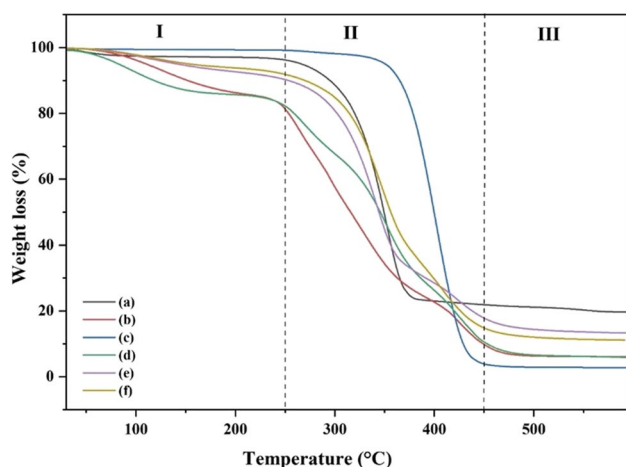


Fig. 3 TGA of cellulose-based composite hydrogel (a) cellulose, (b) PVA gels, (c) PEGDA, (d) PVA-PEGDA gels, (e) PVA-cellulose gels, and (f) PVA-cellulose-PEGDA gels

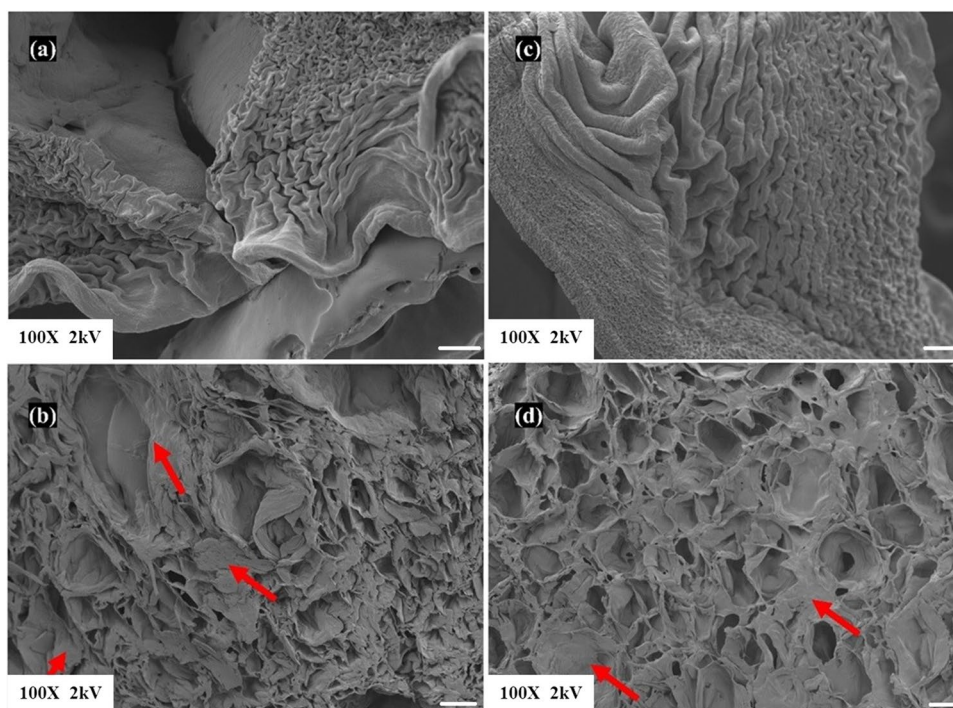
and C-O stretching, respectively. These peaks were similar to previous literature [30].

As shown in Fig. 2, X-ray diffraction was employed to investigate the crystallinity of cellulose-based composite hydrogel. The pristine cellulose, PVA, PEGDA, and PVA-PEGDA gels were provided for comparison. The characteristic peak of composite hydrogel was similar to pristine PVA and cellulose. No evidence of a PEGDA peak can be observed. It can be indicated that PVA and cellulose were the majority part of the composite. PEGDA as a minority part was integrated into PVA. In the case of composite

hydrogel, the peaks were presented at the diffraction angle of 19.36° , 23.04° , and 40.78° . These peaks exhibited the similar level of intensity compared to pristine PVA. These peaks were relatively indexed to diffraction plane of (110), (200), and (220), respectively, as reported in previous literature [31]. However, the peaks belonging to PEGDA exhibited low intensities. It can be implied that PEGDA presented less percent of crystallinity. This was in contrast to cellulose. The diffraction peaks at 2θ of 15.64° , 22.06° , and 26.81° were presented. These peaks were corresponded to diffraction plane of (110), (200), and (004), respectively. This result was in agreement with previous articles [32, 33]. The presence of the (200) and (004) diffraction planes in the cellulose-based composite hydrogels corresponded to hydrogen bonding via irradiation [24, 25]. Therefore, irradiation was an optimal technique to form cellulose-based composite hydrogels, which reduced production processes such as freeze-drying. This was in agreement with the previous article of Chen et al. [34].

In order to define the thermal stability of cellulose-based composite hydrogel, TGA was employed. Figure 3 illustrates the thermal decomposition behavior of composite. It can be categorized that based on the temperature range, thermal decomposition behavior can be classified into three distinct regions. From ambient temperature to 250°C , only 10% of weight loss was observed. Composite was thermally stable within this temperature range. A small amount of weight loss may typically refer to evaporation of water. After that, within the temperature region of $250\text{--}450^\circ\text{C}$, broad region of weight loss was determined. This was probably due to the

Fig. 4 SEM of cellulose-based composite hydrogel **a** PVA gels, **b** PVA-cellulose gels, **c** PVA-PEGDA gels, and **d** PVA-cellulose-PEGDA gels



fact that cellulose-based composite hydrogel is composed of organic molecule. It was combusted and changed to volatile gas such as CO_2 . However, it can be observed that with the presence of cellulose, the characteristic curve was slightly shifted to higher based on the applied external heat. The role of cellulose was significantly provided the superiority of thermal resistance. This result was in agreement with previous literatures [35, 36]. Cellulose can create both intra and intermolecular hydrogen bonds throughout the hydrogel network through irradiation [24, 25, 37]. Furthermore, with the existence of PEGDA, the weight loss was very low. It can be implied that PEGDA offered high thermal stability. Then, when the temperature was superior to $450\text{ }^\circ\text{C}$, weight loss was constant. The thermal degradation was terminated. The rest of weight loss was typically involved to char and residual.

After that, microstructural properties were investigated by scanning electron microscope technique. Figure 4 reports the morphological properties of the cellulose-based composite hydrogel. The sample was prepared by freeze-dry technique in order to remove the presence of water. The presence of cellulose was indicated as a red arrow. It was surrounded by polymer matrix. The neat PVA and PVA/PEGDA binary blend were provided for comparison. It exhibited as a porous structure throughout the hydrogel network. The pore was presented as an interconnected pore with air-instituted in between. This was probably due to the fact that the water is sublimated. With the existence of cellulose, the size of the pore was less ($126.4\text{ }\mu\text{m}$). It can be discussed that the role of cellulose can effectively form the hydrogen bonding with both of PVA and PEGDA. It was typically referred to the fact that $\bullet\text{OH}$ radicals generated during irradiation reacted to form a three-dimensional network structure [24, 25]. It may significantly offer the benefit for dimensional stability such as swelling behavior [38] and compressive strength [39].

After that, in order to employ cellulose-based hydrogel composite as a platform for chemical sensor, the physico-chemical properties of the composite were therefore evaluated. Figure 5 reports the gel fraction and porosity of cellulose-based hydrogel composite. From the fundamental point of view, the hydrogel samples were divided into two parts consisting of water and gel content. For the PVA gels, PVA-PEGDA gels, PVA-cellulose gels, and PVA-cellulose-PEGDA gels, it was noted that the gel fraction increased with radiation dosage (see Fig. 5A). It slightly increased from 10 to 20 kGy, and then it presented as a plateau. It was noted that during exposure to gamma rays, free radicals were formed. It was subsequently provided the effect to both PVA and cellulose. They were cross-linked and polymerized in between [24, 25]. It was also reported that the gel fraction was influenced by the PEGDA. It was commonly known that PEGDA was considered as a water-soluble prepolymer. It can be induced to be crosslinked when gamma irradiation

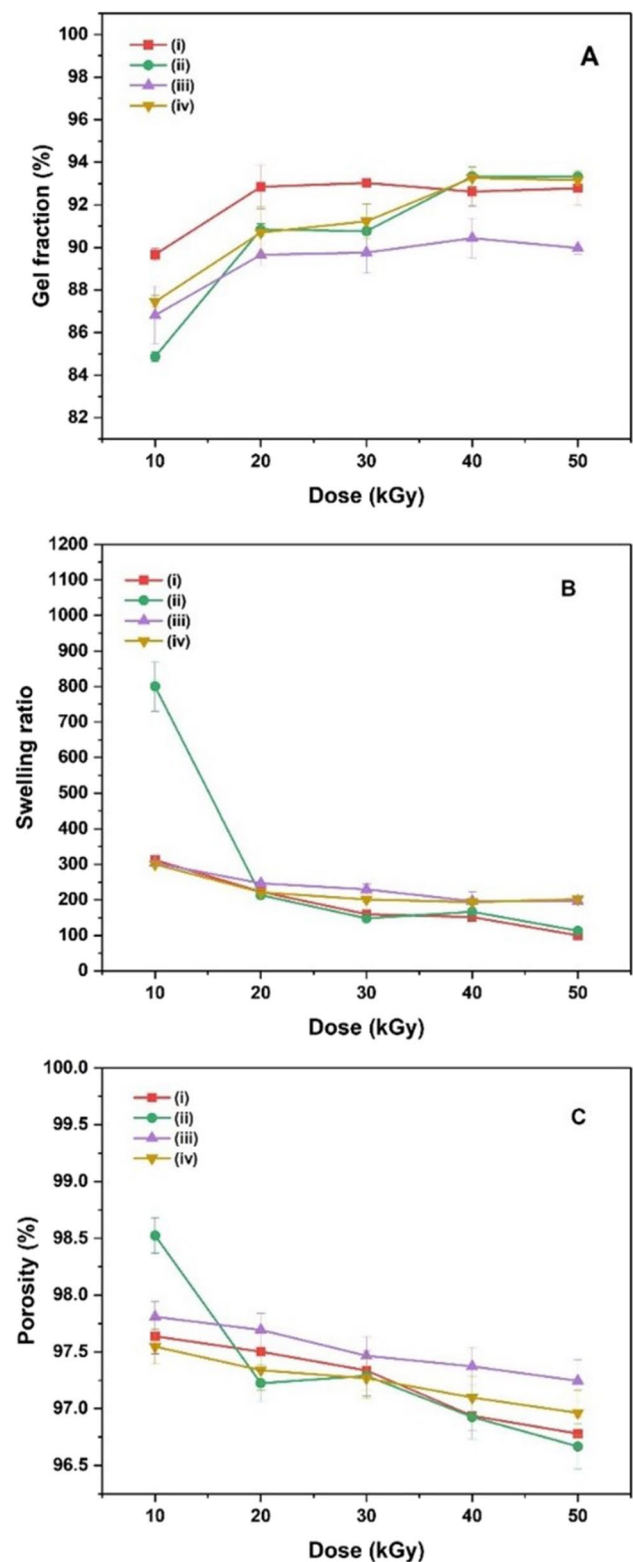


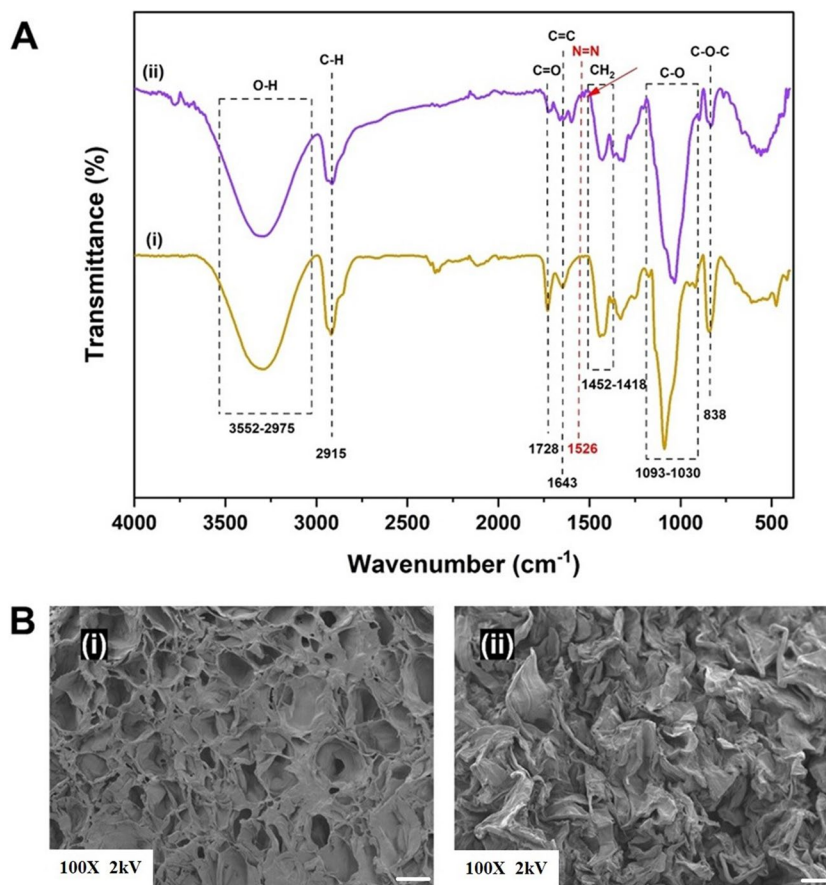
Fig. 5 **A** Gel fraction, **B** swelling behavior, and **C** porosity of (i) PVA gels, (ii) PVA-PEGDA gels, (iii) PVA-cellulose gels, and (iv) PVA-cellulose-PEGDA gels

Table 1 Compressive strength (MPa) of cellulose-based composite hydrogel PVA gels, PVA-PEGDA gels, PVA-cellulose gels, and PVA-cellulose-PEGDA gels

Dose (kGy)	PVA gels	PVA-PEGDA gels	PVA-cellulose gels	PVA-cellulose-PEGDA gels
10	23.22 ± 0.06	20.98 ± 1.51	24.00 ± 1.86	20.81 ± 3.60
20	8.53 ± 2.31	7.35 ± 1.52	15.20 ± 0.86	16.64 ± 1.45
30	9.58 ± 0.51	9.03 ± 1.55	19.02 ± 2.54	23.74 ± 0.20
40	9.95 ± 1.07	12.58 ± 2.44	20.67 ± 2.52	23.81 ± 1.75
50	12.66 ± 1.17	13.93 ± 0.90	21.19 ± 4.01	25.47 ± 0.58

was applied during suspension form [40]. Therefore, the gel fraction therefore increased when PEGDA was added to the hydrogel [41]. The swelling behavior of cellulose-based composite hydrogel is shown in Fig. 5B. The swelling behavior was relatively high when a low gamma irradiation dose was employed. The trend of this behavior was low with respect to high dose. This was probably due to the fact that a high irradiation dose may induce to occur the crosslinking reaction in between hydrogel composite network, suggesting that high dimensional stability was obtained. As shown in Fig. 5C, the porosity of the PVA gels, PVA-PEGDA gels, PVA-cellulose gels, and PVA-cellulose-PEGDA gels were plotted as a function of the radiation dose. The porosity for

all hydrogels decreased as radiation exposure increased. As a result of the mechanism of the crosslinking of polysaccharide derivatives in water, transient reactive species, including hydrated electrons (e^-_{aq}), hydrogen atoms ($\bullet H$), and hydroxyl radicals ($\bullet OH$), were formed during the radiolysis of water [42]. This increased the interaction with hydroxyl radicals ($\bullet OH$) to form crosslinks of hydrogels, resulting in smaller pore size. In addition, PEGDA also contributed to the pore size decrease. Due to PEGDA's interactions with the hydroxyl radical ($\bullet OH$) of the PVA and cellulose chains, the three-dimensional network structure was produced [43]. This was consistent with the SEM images shown in Fig. 4.

Fig. 6 A FTIR spectra and B SEM microstructure of (i) PVA-cellulose-PEGDA gels and (ii) PVA-cellulose-PEGDA-MR gels

The compressive strengths of PVA gels, PVA-PEGDA gels, PVA-cellulose gels, and PVA-cellulose-PEGDA gels are shown in Table 1. The investigation was conducted based on various gamma irradiation doses. The compressive strength for all hydrogels is typically presented in the similar level. It was observed that the compressive strength of hydrogel depends on cellulose. With the presence of cellulose, it was subsequently high. Also, it depended on the gamma irradiation dose. The role of gamma ray resulted in hydroxyl radicals' formation. It can be reacted with cellulose and PVA in order to form a hydrogel network. Therefore, when low gamma irradiation dose was employed, the compressive strength was relatively inferior.

3.2 Preliminary test of hydrogel as a colorimetric sensor

In order to test the hydrogel composite as a platform for colorimetric sensor, MR was integrated into hydrogel as a color agent. Figure 6 reports the FTIR spectra and SEM microstructure of the hydrogel composite with the presence of MR. The peak pattern of FTIR is typically presented in the similar feature. This was probably due to the similarity of the functional group compared to hydrogel. The characteristic peak at a wavenumber of 3400 cm^{-1} was observed. This was attributed to O-H stretching. The peaks at 2800 cm^{-1} and 1700 cm^{-1} were presented due to C-H stretching and C-C stretching, respectively. Furthermore, the peak at

a wavenumber of 1200 cm^{-1} was existed. This peak was corresponded to C-O stretching. Furthermore, in the case of MR, low intensity of peak at 1526 cm^{-1} was presented. This was typically referred to as N-N stretching. This was in agreement with a small amount of MR [44]. In the case of SEM microstructure, the morphological properties were typically presented in the similar feature. The presence of MR was inserted into the porous network of hydrogel.

In order to evaluate the role of methyl red as a color agent, UV-vis spectroscopy was employed. Figure 7 presents the photo-image of MR solution based on various pH ranges (Fig. 7A) and concentrations of NH_3 (Fig. 7C). The red color was presented in the acidic region and at low concentration, while the yellow color was presented in the basic region and at high concentration. Furthermore, based on the wavelength of absorbance, the characteristic peaks were presented at 430 nm and 528 nm. The intensity of the peak typically exhibited a similar trend as the photo-image. These peaks referred to yellow and red color, respectively. The change of color was reported due to the presence of OH^- concentration. This ion was considered as a strong nucleophile [45]. The existence of OH^- ion reacted to the reactive site of methyl red, forming a basic form of COO^- groups (In^-). The yellow color was therefore observed. Furthermore, on the other hand, with the increment of NH_3 concentration, the color was changed from red to yellow. The characteristic peaks of 425 nm and 525 nm were observed due to yellow and red color, respectively.

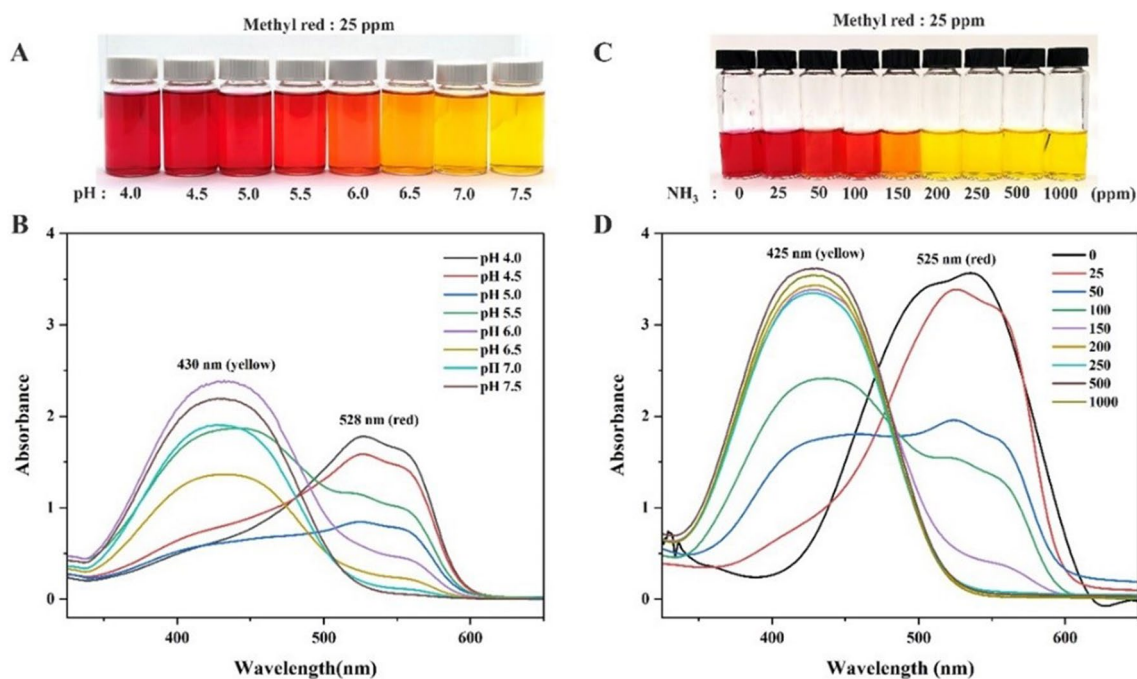


Fig. 7 A, C Color changes and B, D UV absorption spectra of the MR indicator solution for various pH values and NH_3 for various concentrations values

Because NH_3 was dissolved in the water, ammonium ions (NH_4^+) and hydroxide ions (OH^-) were formed. As the OH^- ions concentration of the system increased, it can be formed COO^- groups in the MR.

The color parameters from the ImageJ software were calculated into G/R signals to determine the color changes at various response times (Fig. 8A). At the initial stage, the color of the hydrogel composite was red within 30 s, then it turned to yellow after 8 min. The change of color was typically related to G/R as reported in Fig. 8B. The brightness and yellowness of the hydrogel were indicated by an increasing G/R value [22]. With respect to the increment of time, the color was therefore significantly changed. This was probably due to the fact that hydrogel contained a high amount of water molecule in its structure. The role of water molecule can induce to attach NH_3 to NH_4^+ ion and OH^- ion [46]. Then, the basic formed (In^-) of MR may occur. The color of hydrogel was consequently changed to yellow.

In order to utilize the hydrogel composite as a platform for colorimetric sensor, the demonstration of durian was therefore tested. Figure 9 presents the change of hydrogel

color with respect to investigation time. Similar to Fig. 8, the color of hydrogel was red at the initial stage, and then it turned to yellow when the increment of time was provided. It can be therefore implied to predict the ripening of durian. This was also associated with the G/R signal as reported in Fig. 9B. From the fundamental point of view, the volatile gas from durian contained sulfur compound. [47, 48]. This gas can be induced to the metabolic acceleration. The color change of the hydrogel was due to the interaction between methyl red and volatile sulfur compounds. This led to MR in the form of a COO^- , which was followed: $\text{C}_{15}\text{H}_{15}\text{N}_3\text{O}_2 + \text{C}_4\text{H}_{10}\text{S}_2 \rightarrow \text{C}_{15}\text{H}_{14}\text{N}_3\text{O}_2^- + \text{C}_4\text{H}_{11}\text{S}_2^+$. The color of the hydrogel was then changed to yellow. The preliminary test with durian was therefore noted that hydrogel composite prepared by gamma irradiation technique can be successfully employed as a platform for colorimetric sensor. Then, it will be provided the great promise that cellulose and PVA-based composite for sensor will be degraded along with durian shell.

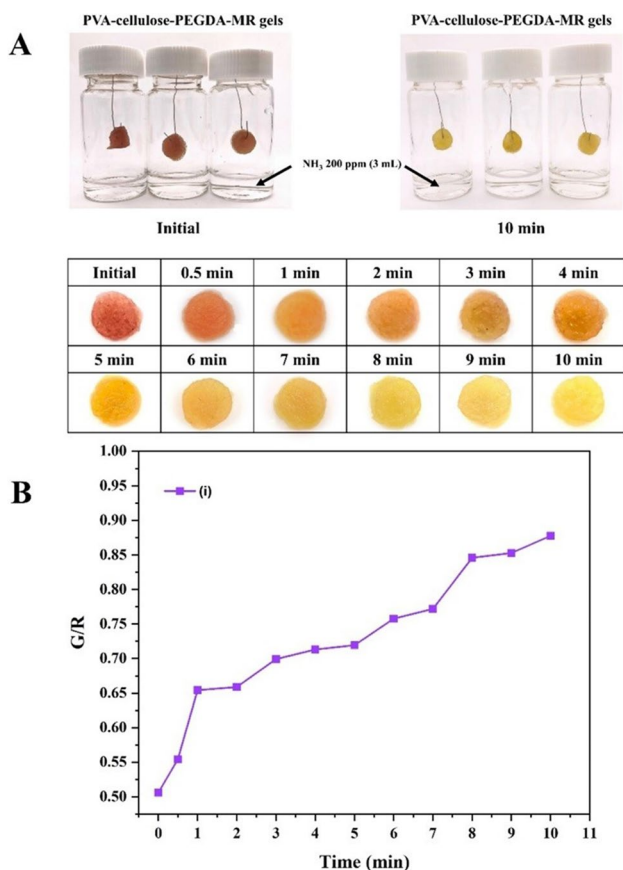


Fig. 8 **A** Color changes of the hydrogel indicator when exposed to ammonia vapor (NH_3) and **B** change in response signal (G/R) versus time of composite hydrogel

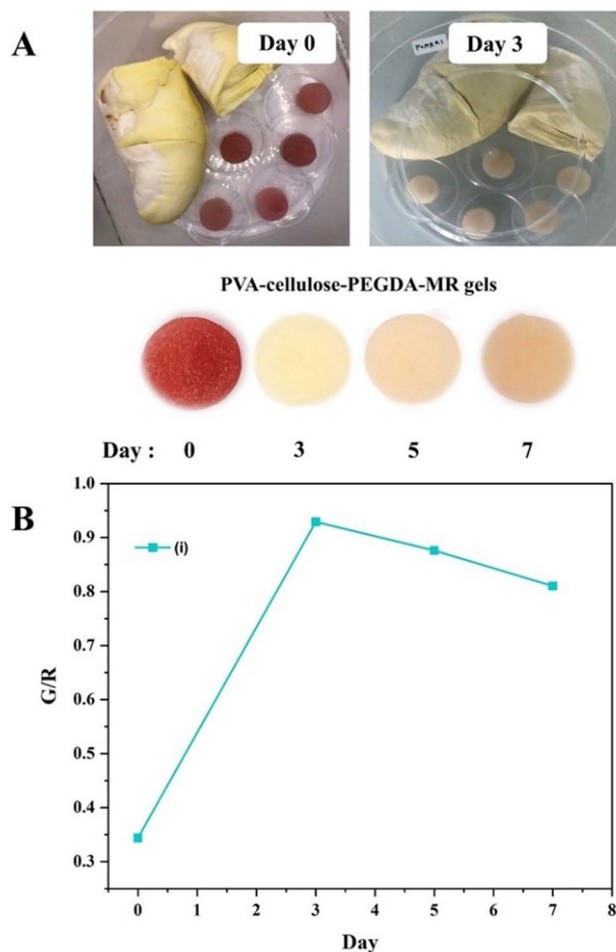


Fig. 9 **A** Color changes and **B** change in response signal (G/R) versus time of (i) PVA-cellulose-PEGDA-MR gels during fresh durian storage at 35 °C

4 Conclusion

Cellulose was successfully extracted from sugarcane bagasse using an alkali treatment and bleaching. The suspension was stirred with NaOH and NaClO₂, respectively. Purified cellulose and PVA-based hydrogel composite were prepared with the weight ratio of 1:1. PEDGA was integrated to facilitate the gel formation. It can be employed as a reinforcement part in composite by gamma irradiation. The irradiation doses were set to be 10–50 kGy. The presence of cellulose did not provide the change of the functional group and crystallinity of the composite. The existence of C-H stretching, O-H stretching, and C=O stretching was observed. These functional groups were belonged to cellulose-based PVA hydrogel composite. The characteristic peaks of the XRD pattern were similar to pristine matrix, suggesting that cellulose was embedded into the matrix network. The role of cellulose significantly offered the superiority of thermal resistance and compressive strength to polymer matrix. It was thermally stable at 200 °C. The compressive strength was in the range of 10–20 MPa. A total of 85–90% of gel fraction, 100–300% of swelling behavior, and 95–97% of porosity were slightly observed. At low irradiation dose, gel fraction was low, while swelling behavior and porosity were relatively high. The role of gamma irradiation can be induced to form the reaction between cellulose and polymer matrix. It can create the •OH radicals to form a three-dimensional network structure. After that, hydrogel composite significantly provided the ability to be employed as a platform for colorimetric sensor. MR was used as dye to react with volatile gas. The characteristic peaks of 425 nm and 525 nm were observed due to yellow and red color, respectively. The color can be changed with respect to time. It was remarkably noted that cellulose and PVA hydrogel composite will be provided the great promise for colorimetric sensor and offered the degradability along with durian shell in the near future.

Acknowledgements This work was mainly supported by the funding under the TINT to University project (2566), Thailand Institute of Nuclear Technology (TINT), Thailand. One (S.U.) of the authors would like to acknowledge the support from the Thammasat University Research Unit in Textile and Polymer Chemistry. This research and innovation activity was funded by the Hub of Talent: Sustainable Materials for Circular Economy, National Research Council of Thailand (NRCT).

Author contribution Nattawan Khiewasawai: conceptualization, methodology

Thitirat Rattanawongwiboon: validation, writing—review and editing, resources

Chonnipha Tangwongputti: validation

Sarute Ummartyotin: writing—original draft, writing—review and editing, supervision, resources

Declarations

Conflict of interest The authors declare no competing interests.

Data availability Data availability can be provided upon request.

References

1. PACK, S., *Sugarcane*. 2010.
2. Y. Snoussi et al., Green, zero-waste pathway to fabricate supported nanocatalysts and anti-kinetoplastid agents from sugarcane bagasse. *Waste Manag.* **155**, 179–191 (2023)
3. J. de Aguiar et al., Enzymatic deconstruction of sugarcane bagasse and straw to obtain cellulose nanomaterials. *ACS Sustain. Chem. Eng.* **8**(5), 2287–2299 (2020)
4. S. Venkatarajan, A. Athijayamani, An overview on natural cellulose fiber reinforced polymer composites. *Mater. Today: Proc.* **37**, 3620–3624 (2021)
5. H.M. Saleh, A.M. Khalil, Plastic films based on waste expanded polystyrene loaded with bagasse powder for packaging applications. *Egypt. J. Chem.* **65**(11), 323–329 (2022)
6. M. Tang et al., Unusual, hierarchically structured composite of sugarcane pulp bagasse biochar loaded with Cu/Ni bimetallic nanoparticles for dye removal. *Environ. Res.* **232**, 116232 (2023)
7. J.-H. Kim et al., Disposable chemical sensors and biosensors made on cellulose paper. *Nanotechnology* **25**(9), 092001 (2014)
8. S.A. Al Kiey, A.M. Khalil, S. Kamel, Insight into TEMPO-oxidized cellulose-based composites as electrochemical sensors for dopamine assessment. *Int. J. Biol. Macromol.* **239**, 124302 (2023)
9. L. Chopra, Extraction of cellulosic fibers from the natural resources: a short review. *Mater. Today: Proc.* **48**, 1265–1270 (2022)
10. C. Sriwong, S. Boonrungsiman, P. Sukyai, Sugarcane bagasse cellulose-based scaffolds incorporated hydroxyapatite for promoting proliferation, adhesion and differentiation of osteoblasts. *Ind. Crop. Prod.* **192**, 115979 (2023)
11. S. Ahmadi, R. Mainali, R. Nagpal, M. Sheikh-Zeinoddin, S. Soleimani-Zad, S. Wang, ... H. Yadav, Dietary polysaccharides in the amelioration of gut microbiome dysbiosis and metabolic diseases. *Obes. Control Ther.: Open Access* **4**(3) (2017)
12. W. Sun, J. Wang, M. He, Anisotropic cellulose nanocrystal composite hydrogel for multiple responses and information encryption. *Carbohydr. Polym.* **303**, 120446 (2023)
13. J. Wu et al., Multiply cross-linked poly (vinyl alcohol)/cellulose nanofiber composite ionic conductive hydrogels for strain sensors. *Int. J. Biol. Macromol.* **225**, 1119–1128 (2023)
14. W. Fang et al., Influence of formic acid esterified cellulose nanofibrils on compressive strength, resilience and thermal stability of polyvinyl alcohol-xylan hydrogel. *Carbohydr. Polym.* **308**, 120663 (2023)
15. H. Baniyadi et al., Ascorbic acid-loaded polyvinyl alcohol/cellulose nanofibril hydrogels as precursors for 3D printed materials. *Mater. Sci. Eng. C* **130**, 112424 (2021)
16. C. Lu et al., Ultra-strong hydroxypropyl cellulose/polyvinyl alcohol composite hydrogel by combination of triple-network and mechanical training. *Int. J. Biol. Macromol.* **184**, 200–208 (2021)
17. A. Ianuzzi, S. Kurtz, 17 - Sterilization of joint replacement materials. *Joint Replacement Technology*, ed. by P.A. Revell. Woodhead Publishing Series in Biomaterials (Woodhead Publishing, 2008), pp 407–427

18. H. Kaouach, γ -irradiation induced effects on structural, morphological and photoluminescence properties of PEO-PVA blended polymer films. *Optik*. **274**, 170563 (2023)
19. P. Chanklinhorm, T. Rattanawongwiboon, S. Ummartyotin, Development of cellulose from sugarcane bagasse and polyacrylamide-based hydrogel composites by gamma irradiation technique: a study of controlled-release behavior of urea. *J. Polym. Environ.* **30**(6), 2631–2641 (2022)
20. S. Sutthasupa, C. Padungkit, S. Suriyong, Colorimetric ammonia (NH₃) sensor based on an alginate-methylcellulose blend hydrogel and the potential opportunity for the development of a minced pork spoilage indicator. *Food Chem.* **362**, 130151 (2021)
21. M.H. Mahaninia, L.D. Wilson, Cross-linked chitosan beads for phosphate removal from aqueous solution. *J. Appl. Polym. Sci.* **133**(5) (2016)
22. Q. Tang et al., Preparation of an aramid nanofiber-reinforced colorimetric hydrogel employing natural anthocyanin as an indicator for shrimp and fish spoilage monitoring. *Eur. Polym. J.* **187**, 111889 (2023)
23. A. Niponsak et al., Novel ripeness label based on starch/chitosan incorporated with pH dye for indicating eating quality of fresh-cut durian. *Food Control* **107**, 106785 (2020)
24. J. Rosiak, P. Ulański, Synthesis of hydrogels by irradiation of polymers in aqueous solution. *Radiat. Phys. Chem.* **55**(2), 139–151 (1999)
25. M.N.K. Chowdhury et al., Radiation processed hydrogel of poly (vinyl alcohol) with biodegradable polysaccharides. *Bio-Med. Mater. Eng.* **16**(3), 223–228 (2006)
26. R. Auta et al., Production and characterization of bacterial cellulose before and after enzymatic hydrolysis. *Afr. J. Biotechnol.* **16**(10), 470–482 (2017)
27. A. Abdulkhali et al., Preparation of cellulose/polyvinyl alcohol biocomposite films using 1-n-butyl-3-methylimidazolium chloride. *Int. J. Biol. Macromol.* **62**, 379–386 (2013)
28. T. Jayaramudu et al., Electroactive hydrogels made with polyvinyl alcohol/cellulose nanocrystals. *Materials* **11**(9), 1615 (2018)
29. T. Jayaramudu et al., Preparation and characterization of hydrogels from polyvinyl alcohol and cellulose and their electroactive behavior. *Soft Mater.* **15**(1), 64–72 (2017)
30. F. Hemmatgir, N. Koupaei, E. Poorazizi, Characterization of a novel semi-interpenetrating hydrogel network fabricated by polyethylene glycol diacrylate/polyvinyl alcohol/tragacanth gum as a wound dressing. *Burns* **48**(1), 146–155 (2022)
31. A.M. Mostafa, A. Menazea, Polyvinyl alcohol/silver nanoparticles film prepared via pulsed laser ablation: an eco-friendly nano-catalyst for 4-nitrophenol degradation. *J. Mol. Struct.* **1212**, 128125 (2020)
32. J. Gong et al., Research on cellulose nanocrystals produced from cellulose sources with various polymorphs. *RSC Adv.* **7**(53), 33486–33493 (2017)
33. N. Montoya-Escobar et al., Use of Fourier series in X-ray diffraction (XRD) analysis and Fourier-transform infrared spectroscopy (FTIR) for estimation of crystallinity in cellulose from different sources. *Polymers* **14**(23), 5199 (2022)
34. M. Chen, P. Cai, Y. Pan, Dual-responsive bagasse cellulose/PVA hydrogels for sustained release of plant growth regulator. *Ind. Crop. Prod.* **195**, 116432 (2023)
35. H. Pingan et al., A silica/PVA adhesive hybrid material with high transparency, thermostability and mechanical strength. *RSC Adv* **7**(5), 2450–2459 (2017)
36. M. Matzen et al., Influence of flame retardants on the melt dripping behaviour of thermoplastic polymers. *Materials (Basel)* **8**(9), 5621–5646 (2015)
37. A. Chami Khazraji, S. Robert, Self-assembly and intermolecular forces when cellulose and water interact using molecular modeling. *J Nanomater* **2013**, 745979 (2013)
38. P. Giusti et al., Hydrogels of poly (vinyl alcohol) and collagen as new bioartificial materials. *J. Mater. Sci. Mater. Med.* **4**(6), 538–542 (1993)
39. R. Santi et al., Modulable properties of PVA/cellulose fiber composites. *J. Appl. Biomater. Funct. Mater.* **17**(1), 2280800019831224 (2019)
40. M. Kozicki, P. Kujawa, J.M. Rosiak, Pulse radiolysis study of diacrylate macromonomer in aqueous solution. *Radiat. Phys. Chem.* **65**(2), 133–139 (2002)
41. Hassan, M., et al., *Swelling and Absorption properties of Polyvinyl Alcohol (PVA) and Acrylic Acid Blend Hydrogels: Effect of γ -Irradiation*. 2016.
42. R.A. Wach et al., Dual stimuli-responsive polysaccharide hydrogels manufactured by radiation technique. *Appl. Sci.* **12**(22), 11764 (2022)
43. Haryanto et al., Fabrication of poly (ethylene oxide) hydrogels for wound dressing application using E-beam. *Macromol. Res.* **22**, 131–138 (2014)
44. P. Balu, I. Asharani, D. Thirumalai, Catalytic degradation of hazardous textile dyes by iron oxide nanoparticles prepared from Raphanus sativus leaves' extract: a greener approach. *J. Mater. Sci. Mater. Electron.* **31**, 10669–10676 (2020)
45. J.-H. Zhang et al., Determination of acid dissociation constant of methyl red by multi-peaks Gaussian fitting method based on UV-visible absorption spectrum. *Acta Phys. -Chim. Sin.* **28**(5), 1030–1036 (2012)
46. Y.H. Kim et al., Non-destructive monitoring of apple ripeness using an aldehyde sensitive colorimetric sensor. *Food Chem.* **267**, 149–156 (2018)
47. Y. Voon et al., Volatile flavour compounds and sensory properties of minimally processed durian (*Durio zibethinus* cv. D24) fruit during storage at 4 C. *Postharvest Biol. Technol.* **46**(1), 76–85 (2007)
48. A. Niponsak, N. Laohakunjit, O. Kerdchoechuen, Contribution to volatile fingerprinting and physico-chemical qualities of minimally processed Durian cv. 'Monthong' during storage: identification of a novel chemical ripeness marker. *Food Bioproc. Tech.* **8**, 1229–1243 (2015)

Springer Nature or its licensor (e.g. a society or other partner) holds exclusive rights to this article under a publishing agreement with the author(s) or other rightsholder(s); author self-archiving of the accepted manuscript version of this article is solely governed by the terms of such publishing agreement and applicable law.